

# QUANTIFYING FORCES IN CELL BIOLOGY

Pere Roca-Cusachs<sup>1,2\*</sup>, Vito Conte<sup>1\*</sup>, Xavier Trepat<sup>1,2,3,4\*</sup>

<sup>1</sup> *Institute for Bioengineering of Catalonia, Barcelona 08028, Spain*

<sup>2</sup> *University of Barcelona, 08028 Barcelona, Spain*

<sup>3</sup> *Institució Catalana de Recerca i Estudis Avançats (ICREA), Barcelona, Spain.*

<sup>4</sup> *Centro de Investigación Biomédica en Red en Bioingeniería, Biomateriales y Nanomedicina, 08028, Barcelona, Spain*

\* Correspondence to: [rocacusachs@ub.edu](mailto:rocacusachs@ub.edu), [vconte@ibecbarcelona.eu](mailto:vconte@ibecbarcelona.eu), [xtrepat@ibecbarcelona.eu](mailto:xtrepat@ibecbarcelona.eu)

**Cells exert, sense, and respond to physical forces through an astounding diversity of mechanisms. Here we review recently developed tools to quantify the forces generated by cells. We first review technologies based on sensors of known or assumed mechanical properties, and discuss their applicability and limitations. We then proceed to draw an analogy between these human-made sensors and force sensing in the cell. As mechanics is increasingly revealed to play a fundamental role in cell function we envisage that tools to quantify physical forces may soon become widely applied in life-sciences laboratories.**

The study of the interplay between physical forces and cell function dates back to well before the term “mechanobiology” was coined. In 1917, D’Arcy Thompson published his celebrated work “On growth and form”, in which he discussed how physical forces contribute to determining the size and shape of living organisms<sup>1</sup>. Even earlier there was evidence that cells sense and adapt to physical forces; for instance, that shear stress controls the size of blood vessels<sup>2</sup> and that mechanical loading causes bone to thicken<sup>3</sup>. Early studies also pioneered tools to apply and measure physical forces in biology at the cellular and subcellular levels. Also in 1917, Chambers developed a micro-needle system to conclude that churning a fertilized sand-dollar egg resulted in the reversible disappearance of the aster<sup>4</sup>. A few decades later, Crick measured material properties of the cytoplasm by developing magnetocytometry tools to twist and drag internalized magnetic particles<sup>5</sup>.

Mechanobiology is thus not a new field but its far-reaching implications and the unexpected diversity of mechanisms have placed it at the forefront of current research<sup>6</sup>. We know today that cells probe their environment through physical forces sufficient to differentiate mesenchymal stem cells<sup>7</sup>, initiate transcriptional programs<sup>8</sup>, drive morphogenesis<sup>9</sup>, direct cell migration<sup>10</sup>, and control malignancy<sup>11</sup>. The mechanisms by which forces mediate these responses have been traditionally attributed to one-step mechanochemical switches located at cell-extracellular matrix (ECM) adhesions<sup>12</sup>, cell-cell adhesions<sup>13</sup>, the plasma membrane<sup>14</sup>, and the nucleus<sup>15</sup>. In analogy with ligand-receptor binding, activation of the mechanochemical switch would trigger a signaling cascade of pure biochemical nature that would leave no downstream role for mechanics. In contrast, current evidence indicates that biochemistry and mechanics constantly cross-talk in mechanotransduction<sup>16, 17</sup>. Thus, a full understanding of

mechanobiology requires the development of tools to measure cellular forces over multiple time and length scales.

We can intuitively understand the concept of force in cell biology in terms of cellular push and pull but we cannot measure force in cell biology as we measure length or time. In fact, we cannot measure force directly in any field of science because Newton's second law defines force as a quantity that can only be indirectly assessed through the direct measurement of other mechanical quantities, such as the material properties and deformations of physical bodies. Consequently, we may only quantify force through force-measurement systems, which are made up of a force sensor and an associated measuring instrument. The force sensor is a physical device that receives in input a physical stimulus related to force and transduces it in a physical quantity directly measurable through the associated instrument. The most familiar force measurement system may be Newton's dynamometer, which at base is a spring scale (the force sensor) that transduces the weight of a mass into a length deformation that we can read through a simple ruler (the associated instrument).

Based on analogous principles, biophysicists have developed systems devised to work as force sensors in cell biology that transduce force into measurable physical quantities such as a mechanical deformation or light. Direct measurement of these physical quantities ultimately allows the quantification of force once the material properties of the force sensor are either known or assumed. In the first section of this review, we focus on techniques based on quantifying the extent to which cellular forces deform inert materials of known mechanical properties (Fig. 1a-c, e-l, Table 1). In the second section, we review techniques that require assumptions of material properties, and we discuss their range of applicability (Fig. 1d, m-t, Table 1). Finally, we draw an analogy between force sensing in the cell and human-made tools to probe physical forces (Table 2). This review focuses on techniques to quantify forces actively generated by cells, thus excluding techniques in which forces are exogenously applied. Hence, we do not discuss magnetic tweezers, optical tweezers, stretchable substrates, fluid flow, or micropipette aspiration, which are often used to either probe cellular responses to force or to measure mechanical quantities such as cell stiffness, rheology, adhesion, surface friction, and fracture stress and refer the reader to excellent recent reviews on these methods<sup>18-20</sup>.

## **Force sensors based on known material properties**

**Traction microscopy.** The earliest technique to measure cellular forces is traction microscopy (Fig. 1a-c, Table 1)<sup>21</sup>. Traction microscopy maps stresses (force per unit area) at the cell surface by measuring deformations of the surrounding material. Virtually every adherent cell that has ever been probed exerts a contractile force upon its underlying 2D ECM-coated substrate. If the substrate is sufficiently soft, the applied force will deform it to a measurable extent. Traction microscopy is based on measuring this deformation by comparing two images of fiduciary markers embedded in the substrate or attached to its surface. The first image is obtained when the cell is applying a force on the substrate (loaded image) and the second when the substrate is fully relaxed (unloaded image or reference image). Recent implementations of this technique involve printing fluorescent markers with regular spacing on the gel surface to avoid the need for a reference image<sup>22, 23</sup>. Image processing algorithms compare the loaded and unloaded images to provide a displacement map (also called displacement field) of the deformed gel, that is, a map that shows the extent to which each pixel of the substrate has shifted from its relaxed position as a consequence of the force exerted by the cell. Typical substrates used for traction microscopy include polyacrylamide or silicon-based gels. Both types of gels are linear elastic and optically transparent, their elasticity can be tuned over several orders of magnitude, and they can be readily coated with ECM<sup>7, 23-25</sup>. A

variety of computational methods can be used to retrieve the traction maps from the displacement field<sup>21, 26-30</sup>. Over time, traction microscopy has been dramatically improved in terms of computation time<sup>26</sup> and spatial resolution<sup>24, 31-33</sup>.

Traction microscopy was originally conceived to compute the 2D force field exerted by a single cell on a 2D substrate<sup>21, 26</sup> but has been extended to multicellular clusters<sup>28</sup> and to 2D substrates of arbitrary stiffness profiles<sup>10</sup>. The 2D approximation is valid in many experimental conditions but cells generally exert 3D forces on 2D substrates, and some cell types exhibit a normal traction component comparable to the in-plane one<sup>34</sup>. 3D forces on 2D substrates (often referred to as 2.5D tractions) can be computed using the same principle described above provided that the displacement field of the substrate is measured in 3D<sup>35-37</sup>.

A far more complicated problem is the computation of 3D traction fields in cells embedded in 3D ECMs. Unlike the 2D and 2.5D cases in which the deformable substrate is tightly engineered by the experimentalist, the 3D ECM is continuously synthesized, degraded, and remodeled by the cell, which precludes a straightforward interpretation of a deformation field in terms of a force field. For example, it is unclear that a large deformation in the vicinity of the cell is caused by a high traction or by local ECM degradation. Moreover, physiological ECMs are composed of fibers with highly non-linear force-extension relationships, and some of these fibers extend whereas others buckle in the same microscopic volume element. To avoid the issues associated with non-linearity and non-affinity of the ECM, Legant et al computed 3D traction fields using synthetic, MMP-cleavable polyethylene glycol (PEG) gels rather than native ECM<sup>38</sup>. Alternatively, Steinwachs et al developed a continuum approach that incorporates non-affine properties of the ECM<sup>39</sup>. The applicability of these 3D traction approaches is still far from that of 2D traction microscopy, but they have already hinted at distinct mechanical behavior in 3D compared to a 2D environment. For example, force applied by MDA-MB-231 breast carcinoma cells appears to be independent of ECM concentration and stiffness in 3D<sup>39</sup>.

Traction microscopy is experimentally straightforward in its simplest applications but its popularity has been limited by the need of advanced software, a limitation now mitigated by the availability of open source codes and ImageJ plugins<sup>40-42</sup>. Nonetheless, there are important experimental caveats. For example, the computational problem of exactly determining the traction field from the displacement field is said to be mathematically ill-posed. This means that the addition of a small amount of measurement noise in the displacement field can lead to a large error in the traction field<sup>42</sup>. Thus, high quality displacement fields are essential and the appropriate data handling through filtering and regularization must be carefully considered for each application. In addition, non-linear and poroelastic models of hydrogel substrates should be progressively incorporated into routine algorithms to improve data quality at large deformations.

**Cantilevers and micropillars.** As an alternative to deformable substrates, contractile surface forces are often measured using cantilevers (Fig. 1e-h, Table 1). Cantilevers are elongated structures with a constant cross section made of an elastic material that are attached to a stiff substrate at one end and free at the other end. A force exerted on the free end causes cantilever bending and, if sufficiently small compared to cantilever length, cantilever displacement and force are proportional. Thus, cell forces can be readily measured from displacements if the proportionality constant (spring constant) is known. Spring constants can be calculated for simple shapes using elasticity theory if the length, shape and stiffness of the material are known or calibrated, for instance by tracking cantilever thermal fluctuations<sup>43</sup>. Microfabrication techniques allow the production of arrays of cylindrical micron-scale cantilevers called micropillars, usually made of polydimethylsiloxane (PDMS)<sup>44-48</sup> or polyacrylamide<sup>49, 50</sup>, that serve as cellular substrates

(Fig. 1e-f). If the pillars are spaced closely enough and their apical surface is selectively coated with ECM, cells attach and exert forces only at the pillar tips. Thus, cell forces can be measured from pillar displacements and mapped at the subcellular level.

This approach has a few advantages over traction microscopy based on continuous substrates. First, displacements can be calculated from undeflected pillar positions in the uniform grid, without requiring a reference image. Second, displacements of a given pillar only depend on the force applied to that pillar, making force calculation simpler and less computationally intensive. Finally, the dependence of stiffness on micropillar geometry allows the generation of heterogeneous mechanical environments without altering material properties<sup>51</sup>, and abrupt changes in pillar shape can generate steep rigidity gradients<sup>52</sup>. Furthermore, magnetic actuators can be inserted in individual pillars to provide additional mechanical stimuli<sup>53, 54</sup>. However, there are also disadvantages. The discrete, rather than uniform, adhesive surface presented to cells greatly influences the morphology of cell-ECM adhesions. Although less of an issue on pillars with sub-micron diameter<sup>47, 48</sup>, the recruitment of integrins and adhesion proteins will be affected by the ECM patterning imposed by the pillars. Additionally, even if some approaches have been proposed<sup>55</sup>, calculating an effective stiffness of such substrates for comparison with physiological conditions is not straightforward. Finally, fabrication technologies restrict the stiffness range (~ 1 order of magnitude) compared with continuum substrates (more than 2 orders), limiting the ability of micropillars to reproduce the wide variations in stiffness found among different types of *in vivo* tissues.

While generally operating at the cellular and tissue levels rather than at the subcellular one, other approaches consist of attaching cells to cantilevers in atomic force microscopes (AFM)<sup>56</sup>, as well as optical<sup>57, 58</sup> or microelectromechanical (MEMS)<sup>59</sup> approaches to measure forces. Despite the loss in spatial resolution, those devices often have the advantage of a precise, real-time conversion of cantilever deflection and force into an electric signal, which also enables the implementation of force feedback systems (Fig. 1g-h).

**Droplets and inserts.** Traction microscopy and cantilever based methods are useful to measure cell-generated surface forces *in vitro* but they are not applicable *in vivo*. A new approach that overcomes this limitation is the insertion of deformable materials of known mechanical properties in the tissue of interest. This method was first demonstrated using micro-injected micron-sized oil droplets of known surface tension coated with adhesion receptors<sup>60</sup> (Fig. 1i,j). Reconstruction of the droplet shape through standard imaging techniques provides a measurement of the anisotropy of the local stresses in the tissue. Combination of oil-droplets with ferrofluids enables not only the quantification of cell-generated forces but also the application of controlled forces<sup>61</sup>. One caveat is that droplet incompressibility prevents a directed measurement of the isotropic component of the stress. Therefore, this technique cannot discern between isotropic pushing and pulling, but it is informative of stress anisotropy. Other limitations are the assumption that surface tension of the droplet be unchanged by its insertion in tissue and the absence of a direct measurement of the shear stress on the droplet. Some of these limitations have been partially overcome by the recent use of hydrogel-based inserts, which allow shear stress measurements as well as absolute stress measurements by virtue of their well-characterized compressibility and poroelasticity<sup>62</sup>.

**Molecular sensors.** The techniques described above provide force maps at the cell surface by measuring deformations of the inert biomaterials that surround the cell. The very same principle can be used at the nano-scale to measure the force borne by a specific molecule; if material mechanical properties can be assessed at the molecular scale, then deformations of individual molecules can be converted into forces.

This principle has been harnessed to generate a wide array of sensors measuring molecular forces<sup>63</sup> (Table 1, Fig. 1k,l). Here the mechanical response (force/extension curve) of molecular domains of choice (linkers) is first determined through single molecule techniques such as AFM or optical tweezers. After this calibration step, linkers are coupled to molecules of interest. As the nanoscale deformations of individual molecules cannot be resolved optically, they are measured indirectly through fluorescence microscopy. In a common implementation, a “cassette” containing a mechanically calibrated linker flanked by two different fluorophores is encoded into a protein of interest. Force application to the molecule causes stretching of the linker, thereby altering fluorescence energy transfer (FRET) between the two fluorophores. The mechanical properties of the linker, for instance an  $\alpha$ -helix<sup>64</sup> or different peptides<sup>65,66</sup>, and the FRET range of the fluorophore pair determine the sensitivity and force range of the sensor, which typically spans from 1 to 10 pN. This approach has been used to quantify forces transmitted across a variety of proteins, including vinculin<sup>66</sup>, talin<sup>67</sup>, E-cadherin<sup>68,69</sup>, VE-cadherin, and PECAM<sup>70</sup>.

If the aim is to measure forces across extracellular ligands such as ECM molecules, sensors can be synthesized and then coupled to cell substrates<sup>71-74</sup> rather than being genetically encoded. This strategy expands the choice of linkers and fluorophores, allowing, for instance, the use of fluorophore/quencher pairs, which increase their fluorescence as they are separated<sup>72,73</sup>. By providing a direct fluorescence measurement rather than a ratiometric one (as in FRET), sensitivity can be dramatically increased. As an alternative to protein domains, DNA hairpin linkers allows for a “digital” readout, displaying whether the threshold to open the molecule has been crossed<sup>72,73</sup>. The force threshold can be controlled by tuning the DNA sequence<sup>75-77</sup>. In addition to DNA, larger and more mechanically stable proteins can be used, enabling the measurement of forces up to the 100 pN range<sup>78</sup>.

In summary, although molecular force probes only quantify the modulus and not the direction of force exertion, they provide fundamental information on force levels experienced by specific molecules. Certain issues remain to be resolved, namely the discrepancy in reported force levels between different approaches<sup>71-73</sup>, the difficulty in precisely inferring forces from molecular extension due to its stochastic nature and its dependence on force loading profiles, and the distinction between average and individual molecular forces. However, this approach opens the door to an enormous wealth of new information on molecular force transmission, potentially fundamental in elucidating molecular mechanisms in mechanobiology.

### **Force sensors based on unknown material properties**

The techniques discussed thus far are based on quantifying the deformation of inert sensors the material properties of which can be characterized. Therefore, these methods provide exact force measurements within the uncertainty of material calibration and measurement noise. A different family of techniques is based on applying static or dynamic force balance principles to cellular structures the mechanical properties of which are unknown. In principle, these techniques are less powerful but they yield reliable results within a range of reasonable assumptions.

**Monolayer stress microscopy.** Soon after the development of traction microscopy it was recognized that knowledge of traction forces was sufficient to compute average intracellular tension using force balance arguments<sup>79</sup>. This idea was later refined to enable the quantification of intracellular and intercellular tension in cell collectives such as cell doublets<sup>80,81</sup>, clusters<sup>82</sup>, and monolayers<sup>28,83-85</sup>. In this review, we refer to this technique as Monolayer Stress Microscopy (MSM). The rationale behind MSM can be

simply illustrated as a tug-of-war. If the (traction) force exerted by each player on the ground is known, then tension everywhere in the rope is fully defined by Newton's laws<sup>86</sup>. Similarly, if traction exerted by a cohesive group of cells is known, then tension at cell junctions is defined. This principle can be extended to a two-dimensional cell system such as a cell monolayer to compute the two-dimensional stress tensor within and between cells<sup>83, 87-89</sup> (Fig. 1d, Table 1). Unlike the unidimensional case, recovery of 2D stress requires assumption of material properties, specifically of the compressibility of the system. This property is generally not accessible, but this may not be an issue as compressibility variations over a reasonable range result in minor changes in the recovered stress tensor<sup>90, 91</sup>. Monolayer stress microscopy thus far has mainly been based on the assumption that monolayers are thin elastic sheets of homogeneous mechanical properties<sup>83</sup>. Recently, this restriction has been lifted by combining traction force maps and imaging of focal adhesions and stress fibers, which allowed quantification of tension carried by each fiber<sup>92</sup>. Because MSM uses traction force maps as an input, the technique is affected by the limitations of traction microscopy in terms spatial resolution and computational costs.

**Laser ablation.** Laser ablation is an established technique in which laser-pulse energy is focused to obliterate biological structures that transmit forces at the subcellular, cellular or tissue level (Fig. 1m-p, Table 1). Different ablation modes include severing cytoskeletal elements<sup>93-95</sup>, intercellular junctions<sup>96-100</sup>, and supracellular cables<sup>101</sup>, as well as obliterating cell cortical networks<sup>102-104</sup> and individual or multiple cells<sup>105-109</sup>. Laser ablation generally causes the expansion of the targeted structure. This indicates that the ablation locus and its surroundings prior to ablation were under tension in the direction opposite to that of expansion – an ablation followed by shrinkage would instead indicate tissue compression. These qualitative considerations can be made quantitative if material properties are known or assumed. Ablated structures usually undergo a damped elastic recoil, that is, the speed of the wound edge exponentially plateaus to zero over a characteristic time interval  $\tau$  (viscosity-to-elasticity ratio)<sup>93, 96, 103, 104</sup>. In such cases, the initial speed of the wound edge provides a local estimate of the tension-to-viscosity ratio whereas the final extent of wound recoil provides a local estimate of the tension-to-elasticity ratio.

Force estimation conducted through laser ablation is limited by the assumption that material properties are constant and uniform across experimental conditions. If these material properties can be determined through independent methods, force measurements through laser ablation may be considered absolute and can also be compared across different biological systems. This could be achieved, for example, by combining laser ablation with non-contact tools to map cell mechanics<sup>110</sup>. Despite these limitations, laser ablation remains a very versatile technique because it allows sampling relative magnitude and direction of tension through multi-scale ablation modes both *in vitro*, *in vivo* and *ex vivo*<sup>97, 99-102, 104, 105, 108, 109</sup>. Moreover, laser ablation may be combined with *in silico* modelling for a more complex assessment of cell and tissue mechanics<sup>93-95, 98, 100, 103-105</sup>. Thus, despite its invasiveness and underlying assumptions regarding material properties, laser ablation is often the technique of choice to infer relative tension levels at cytoskeletal fibres and cell junctions.

**Geometric force inference.** When combined, all forces arising in cells and tissues must equilibrate inertial forces at all times (Newton's second law). These forces may include cellular cortical tensions, elastic forces associated with subcellular components, pressures generated by the inner cytoplasm and frictional responses to deformation. In the vast majority of experiments at cell and tissue level, inertia is negligible and cell forces equilibrate each other by adding up to naught. If motions of cells and tissues are also slow enough, viscous forces too will be negligible with respect to all other forces defining the physics of the biological system. Furthermore, biophysical quantifications often extend over time scales long enough for cellular poroelastic effects to be irrelevant<sup>111</sup>. With these assumptions in mind, a static force-balance of only two primary forces can account for the mechanics of cells and tissues: intracellular

pressures and cellular cortical tensions<sup>112-119</sup>. On a first level of approximation, intracellular pressures and cortical tensions can be assumed to be uniform within each cell and over cell membrane segments between consecutive intercellular junctions.

Such biomechanical understanding of cells is the foundation of a class of techniques known as the geometric force-inference methods (Fig. 1q-t, Table 1). Under the physical assumptions mentioned above, these methods are independent of the specific material properties of cells and tissues, including whether these are (poro)-elastic, viscous or viscoelastic<sup>111</sup>. This methodology consists in measuring the angle at which cell membranes join double- and triple- junctions with their neighbours. Forces are inferred from deviation of these angles from their equilibrium configuration. Cell boundaries and angles can be determined through segmentation of microscopy images, a feature that makes force inference techniques non-invasive. However, this class of techniques can only infer forces providing a relative rather than absolute value.

Force inference approaches have evolved to tackle issues affecting the technique, which mostly concern the stability of the solution process and its sensitivity to noise – including that due to image segmentation<sup>112-118</sup>. These problems could be addressed through advanced equation solvers and modified assumptions about the forces involved in the biological process being quantified. A significant advancement in addressing these problems ensued from allowing the edge-lines segmenting cell boundaries to be curved<sup>112</sup>. Recent geometric improvements in force inference methods enable force quantification in 3D, as well as addressing biological contexts where it is not possible to assume slow motions and neglect viscous forces<sup>120</sup>. Fitting dynamic models of cell mechanics to quantitative data of cell shape and cytoskeleton flows has enabled force inference during polarization of *C. Elegans* embryos<sup>121</sup> and cell division<sup>122</sup>. Despite underlying assumptions, force inference methods are not invasive and, as such, they are preferred to laser ablation methods to quantify relative forces during dynamic processes *in vivo*.

### **The cell as a force sensor**

The most relevant force sensor in biology is not a device fabricated in a laboratory by scientists; rather, it's the cell itself. How cells sense forces is a research topic in itself that has been extensively reviewed elsewhere<sup>123-125</sup>. However, it is worth highlighting the analogy between human-made and “cell-made” force sensors, and to briefly address how the latter can be studied experimentally (Table 2). As in the research tools described above, cellular force sensors require materials having known properties and becoming deformed in a specific way on force application. Although some studies have suggested that cellular force sensors could involve the entire cell cytoskeleton<sup>46</sup>, they are generally assumed to consist of local molecular structures that change conformation when force is applied. These molecular structures are comparable to the molecular force sensors described above with one key difference: instead of leading to the emission of light, force application alters their conformation and changes their activity or affinity for binding partners. Conformational changes include molecular extension<sup>126</sup>, domain reorientation<sup>127</sup>, unfolding of previously folded domains<sup>128</sup>, bond rupture<sup>129</sup> and opening of ion channels<sup>130, 131</sup>. The study of such force-induced molecular conformational changes has exploded due to the development of nanotechniques allowing precise mechanical manipulation of single molecules through, for instance, AFM or magnetic and optical tweezers. This has allowed the *in vitro* study of the mechanosensing properties of cytoskeletal proteins like talin<sup>128, 132</sup>,  $\alpha$ -catenin<sup>133</sup>, or titin<sup>134</sup>, among many others. A significant challenge is the measurement of such conformational changes within live cells. Although correctly isolating single molecule interactions within cells can be problematic, this can be achieved for

membrane-bound proteins with extracellular domains accessible to external probes. For instance, AFM and biomembrane force probe techniques have been used to study how force affects integrin extension<sup>126</sup>, the dissociation of integrin-ECM bonds<sup>135</sup> and the unfolding of glycoproteins<sup>136</sup>.

The precise measurement of force-induced conformational changes in intracellular molecules remains a significant problem, although different approaches have been proposed. Margadant et al.<sup>137</sup> labelled the two ends of talin molecules with different fluorophores to monitor talin extension *in vivo*. However, conclusively identifying which fluorophore pairs correspond to the same molecule is non-trivial, and involves various assumptions and intensive image processing. Similarly, Rivas-Pardo et al.<sup>134</sup> labelled specific domains of titin within sarcomeres using quantum dots, and then harnessed the large size of the titin molecules to resolve the separation between quantum dots and monitor their extension. The Vogel group<sup>138, 139</sup> labeled domains of the ECM protein fibronectin with FRET fluorophore pairs, demonstrating protein extension in response to force. Krieger et al.<sup>140</sup> used a cysteine shotgun technique to specifically label cysteine residues, and found that cysteine labelling in several proteins was altered after mechanical stimuli in live cells. Because cysteine is often buried within the tertiary or quaternary protein structure, this is indicative of force-induced conformational changes leading to cysteine exposure. Finally, electron microscopy images of cellular cryosections have been used to detect tension-induced conformational changes in membrane structures like caveolae<sup>14</sup>. In all those techniques, comparisons of different conditions submitted or not to mechanical forces are essential to assess whether the detected conformational changes are indeed force-induced. However, it is often difficult to completely rule out other causes, or to distinguish whether forces affect the protein under study directly or downstream of a mechanosensing cascade. Recently, we have proposed an alternative method to evaluate the role of molecular mechanics by introducing mutations previously demonstrated to affect talin mechanical unfolding at the single molecule level *in vitro*<sup>141</sup>. By comparing the effect of wild type talin versus the mechanical mutant, it was possible to isolate the effects mediated specifically by force-induced talin unfolding<sup>16</sup>.

Since cell responses to mechanical signals involve complex signaling cascades, whether and how cells respond to forces can be assessed by measuring downstream events. Typical force sensitive events include changes in focal adhesion dynamics<sup>142, 143</sup>, membrane currents triggered by mechanosensitive channels<sup>144</sup>, activation of effectors such as src<sup>145</sup> or vinculin<sup>146</sup>, and nuclear localization of mechanosensitive transcriptional regulators<sup>147</sup>. Additionally, the cell response can be studied after application of external forces through devices such as magnetic or optical tweezers<sup>148-150</sup>. However, it is important to note that such techniques, while providing fundamental information on mechanosensitive cascades, do not directly assess the specific mechanism by which cells sense forces.

## Conclusions and outlook

The past two decades have seen the development of a wide variety of techniques to probe cell-generated forces. These techniques have revealed an unanticipated variety of mechanisms through which cells move, differentiate, divide, remodel, flow, and sense their microenvironment. These mechanisms are now known to operate at multiple length scales ranging from molecular forces that unfold cryptic protein domains to long-ranged supra-cellular force patterns that govern collective cell migration and wound healing. Physical forces are no longer seen as simple switches of mechanotransduction but also as mechanisms to propagate information within and between cells.

In this review, we have provided an overview of current techniques to quantify cell-generated forces. The most reliable of such techniques are those based on measuring the deformation of materials with known



properties (Fig. 1a-c, e-l, Table 1). However, these techniques are generally restricted to *in vitro* systems and they are sometimes affected by low signal-to-noise ratios. Alternatively, cell-generated forces can be inferred by using techniques that require a set of mechanical assumptions such as laser ablation or geometric force inference (Fig. 1d, m-t, Table 1). Whereas these techniques are, in principle, less desirable than those based on sensors of known mechanical properties, they are often the only choice to access forces at cell junctions, at cytoskeletal fibers and *in vivo*. Quantification using these techniques is reliable, provided underlying assumptions are correctly assessed for each specific experimental condition.

Besides the nature of the sensor and the associated mechanical assumptions, the investigator will need to consider several factors before opting for one technique over the other. These may include: whether the sample is *in vivo* or *in vitro*, in 2D or 3D, and physically accessible for contact; whether absolute force values are required or relative ones suffice; whether the process is dynamic and requires time lapse measurements, or a one-off time point quantification is sufficient (even at the cost of destroying the sample). In addition, spatial resolution (nano-scale vs micro-scale) and force resolution (from the piconewton scale to hundreds of nanonewtons) need to be carefully analyzed. With these considerations in mind, the reader is referred to Table 1 of this review to identify the techniques suited to best address a particular scientific question.

We currently have access to a wide repertoire of techniques to probe cellular forces, but these techniques still require specialized skills and are yet far from becoming routine laboratory tools. The simplest techniques, such as traction force microscopy to probe cell-ECM forces *in vitro*, are rapidly leading the way towards standardization through reproducible experimental protocols and open-source software. Other tools, such as molecular force sensors, hold promise for force quantification *in vivo*, but are still affected by calibration issues and low signal-to-noise ratio. In light of the increasing realisation of the importance of mechanobiology in life sciences, it is not unreasonable to imagine that force measurement tools will become as standard as those to measure gene expression and protein concentrations.

## Acknowledgments

We apologize to the many colleagues whose work could not be cited owing to space constraints. We thank M. Arroyo, J.C. del Álamo, J.J. Muñoz, G.W. Brodland, and all members of our laboratories for critical comments and encouragement. The authors acknowledge support by the Spanish Ministry of Economy, Industry and Competitiveness through the Centro de Excelencia Severo Ochoa Award to the Institute of Bioengineering of Catalonia, and through grants BFU2015-65074-P to XT, BFU2014-52586-REDT and BFU2016-79916-P to PR-C, and BFU2016-75101-P and RYC-2014-15559 to V.C. The authors also acknowledge support by the Generalitat de Catalunya (Cerca Program and 2014-SGR-927 to XT), the European Research Council (CoG-616480 to XT), the European Commission (project 731957 to PR-C and XT) and Fundació la Marató de TV3 (project 20133330 to PR-C).

**Conflict of interest:** The authors have no competing financial interests.

## Figures

### Figure 1. Force quantification techniques for cell biology.

(a-d) 2D Traction microscopy and Monolayer Stress Microscopy (reproduced with permission from ref. 90). (a) Phase contrast microscopy of migrating MDCK cells (scale bar is equal to 50  $\mu\text{m}$ ). (b) Superposition of micro-beads images in the substrate underlying cells during migration (pseudo-coloured in green in the inset) and after cell removal via trypsin (pseudo-coloured in red in the inset). (c) Traction forces along the x-axis of the cells shown in (a). (d) Inter- and intracellular stresses (xx-component of the epithelial stress tensor). (e-f) Micropillars (reproduced with permission from reference 44). Scanning electron micrographs of a micropillar array without cells (e) and with an adhered smooth muscle cell (f). Scale bar is equal to 10  $\mu\text{m}$ . (g-h) Cantilevers (reproduced with permission from reference 151). Images of a C2.7 cell adhered to a rigid substrate at the bottom and to a flexible plate (cantilever) at the top. After the cell establishes initial contact (g) it adheres to both substrates and exerts contractile force (h), deflecting the cantilever. (i-j) Inserts (reproduced with permission from reference 60). (i) Confocal section through an aggregate of GFP-positive tooth mesenchymal cells (green) containing fluorocarbon droplets (red) coated externally with ligands for integrin receptors. (j) 3D reconstruction of fluorocarbon droplets showing values of the anisotropic stresses mapped on the droplet surface. (k-l) Molecular sensors (reproduced with permission from reference 66). Colormap images displaying the FRET index in a transfected vinculin force-sensor and localized to cell-ECM adhesions (k with insets in l). Low index indicates high force. Scale bar is 20  $\mu\text{m}$ . (m-p) Laser Ablation (reproduced with permission from reference 95). Incision of a stress fiber in living cells through laser nanoscissor. (m) A laser nanoscissor severs a single stress fibre bundle in an endothelial cell expressing EYFP-actin (arrowhead indicates the position of the laser spot; bar is equal to 10 $\mu\text{m}$ ). (n-p) Ends of the severed stress fibre (inset in p) splay apart over a period of 15 seconds. (q-t) Force Inference (adapted with permission from reference 152). (q) Cells from the amnioserosa and adjacent lateral ectoderm (upper left corner) of a Bownes stage 13 *Drosophila* embryo. (r) Watershedding is used to segment the image to obtain cell boundaries. (s) Circular fitting is used to determine edge curvatures and edge tangent angles at the triple junctions. (t) The force-inference equation sets are solved and edge tensions and inner cell pressures are computed in relative units. Color bars refer to (t).

## Tables

**Table 1: Summary of techniques to measure cellular forces.** *2D Traction microscopy.* A cell (pink) is laid on a hydrogel (orange) embedded with microbeads (grey). Traction forces (blue) exerted by adherent cell (magenta) are computed from displacement (green) of the bead (black). *3D Traction microscopy.* A cell (pink) is embedded on synthetic or native ECM containing microbeads (grey). Traction forces (blue) exerted by the cell (magenta) are computed from displacement (green) of the bead (black). *Micropillars.* A cell (pink) is laid on micropillars at rest (grey). Traction forces (blue) exerted by adherent cell (magenta) are computed from the displacement (green) that they induce by bending the pillar (black). *Cantilevers.* A cell (pink) is laid on a plate (orange) underneath an AFM cantilever (grey). The deforming cell (magenta) exerts forces (blue) that can be computed through displacement (green) of the deformed cantilever (black). *Inserts.* An undeformed insert (grey) is introduced in a cell aggregate (pink). Cell forces (blue) exerted by migrating or stretched cells (magenta) are computed from deformation (green) of the insert (black). *Molecular sensors.* Cell features (pink) are connected to a linker molecule (grey). Moving cell features (magenta) exert cell forces (blue) that can be computed through FRET (green) of the stretched linker molecule (black). *Monolayer Stress Microscopy.* Interconnected cells (magenta) equilibrate cell-substrate

tractions (green) through intercellular stresses (blue). *Laser Ablation*. Diverse features (grey) in cells (pink) – specifically filaments in this illustration – may be severed through short and intense laser pulses (orange). Deformation (green) of the wounded feature (black) of these cells (magenta) – displacements of retracting fibre in this specific example – are used to compute tension (blue). *Force Inference*. Cell edges (pink) in equilibrium at triple junctions are displaced (magenta) by inter and intra cellular forces (blue). Angle variations (green) with respect to the equilibrium configuration are used to estimate cellular forces.

**Table 2: The cell as a force sensor.** *Cytoskeleton*. A cell (pink) responds to different forces (blue) transmitted to their substrate by reorganizing their cytoskeleton (grey/black). *Molecular extension/unfolding*. A molecule is in a folded/bent configuration (grey), but under force (blue) extends and exposes a binding site (black) to another molecule (green). *Domain reorientation*. A molecule (pink) changes conformation under force (blue), altering the affinity for a binding partner (black). *Bond rupture*. A bond between two molecules (grey) breaks under force (black). This bond can be intracellular, intercellular, or link cells (in pink) to their surrounding ECM as shown in scheme. *Opening of ion channels*. An ion channel on the cell membrane (pink) changes conformation under force (membrane tension, blue), altering its ability to transport ions (grey/black).

## Bibliography

1. Thompson, D.A.W. *On Growth and Form*, Edn. 2. (Cambridge Univ. Press, Cambridge; 1942).
2. Murray, C.D. The Physiological Principle of Minimum Work: II. Oxygen Exchange in Capillaries. *Proc Natl Acad Sci U S A* **12**, 299-304 (1926).
3. Wolff, J. *The Law of Bone Remodeling*. (Berlin Heidelberg New York: Springer, 1986 (translation of the german 1892 edition)).
4. Chambers, R. Microdissection studies II the cell aster a reversible gelation phenomenon. *J Exp Zool* **23**, 483-505 (1917).
5. Crick, F.H.C. & Hughes, A.F.W. The physical properties of cytoplasm. *Exp. Cell. Res.* **1**, 37-80 (1950).
6. Paluch, E.K. *et al.* Mechanotransduction: use the force(s). *BMC Biol* **13**, 47 (2015).
7. Engler, A.J., Sen, S., Sweeney, H.L. & Discher, D.E. Matrix elasticity directs stem cell lineage specification. *Cell* **126**, 677-689 (2006).
8. Farge, E. Mechanical induction of Twist in the Drosophila foregut/stomodaeal primordium. *Current biology : CB* **13**, 1365-1377 (2003).
9. Bosveld, F. *et al.* Mechanical control of morphogenesis by Fat/Dachsous/Four-jointed planar cell polarity pathway. *Science* **336**, 724-727 (2012).
10. Sunyer, R. *et al.* Collective cell durotaxis emerges from long-range intercellular force transmission. *Science* **353**, 1157-1161 (2016).
11. Miroshnikova, Y.A. *et al.* Tissue mechanics promote IDH1-dependent HIF1alpha-tenascin C feedback to regulate glioblastoma aggression. *Nature cell biology* **18**, 1336-1345 (2016).
12. Rivelino, D. *et al.* Focal contacts as mechanosensors: externally applied local mechanical force induces growth of focal contacts by an mDia1-dependent and ROCK-independent mechanism. *J Cell Biol* **153**, 1175-1186 (2001).
13. Yonemura, S., Wada, Y., Watanabe, T., Nagafuchi, A. & Shibata, M. alpha-Catenin as a tension transducer that induces adherens junction development. *Nature cell biology* **12**, 533-542 (2010).
14. Sinha, B. *et al.* Cells respond to mechanical stress by rapid disassembly of caveolae. *Cell* **144**, 402-413 (2011).
15. Swift, J. *et al.* Nuclear lamin-A scales with tissue stiffness and enhances matrix-directed differentiation. *Science* **341**, 1240104 (2013).
16. Elosegui-Artola, A. *et al.* Mechanical regulation of a molecular clutch defines force transmission and transduction in response to matrix rigidity. *Nature cell biology* **18**, 540-548 (2016).
17. Schwarz, U.S. & Gardel, M.L. United we stand: integrating the actin cytoskeleton and cell-matrix adhesions in cellular mechanotransduction. *J Cell Sci* **125**, 3051-3060 (2012).
18. Polacheck, W.J. & Chen, C.S. Measuring cell-generated forces: a guide to the available tools. *Nature methods* **13**, 415-423 (2016).
19. Sugimura, K., Lenne, P.F. & Graner, F. Measuring forces and stresses in situ in living tissues. *Development* **143**, 186-196 (2016).
20. Campas, O. A toolbox to explore the mechanics of living embryonic tissues. *Semin Cell Dev Biol* **55**, 119-130 (2016).
21. Dembo, M. & Wang, Y.L. Stresses at the cell-to-substrate interface during locomotion of fibroblasts. *Biophys J* **76**, 2307-2316. (1999).
22. Polio, S.R. *et al.* Topographical control of multiple cell adhesion molecules for traction force microscopy. *Integr Biol (Camb)* **6**, 357-365 (2014).
23. Bergert, M. *et al.* Confocal reference free traction force microscopy. *Nature communications* **7**, 12814 (2016).

24. Han, S.J., Oak, Y., Groisman, A. & Danuser, G. Traction microscopy to identify force modulation in subresolution adhesions. *Nature methods* **12**, 653-656 (2015).
25. Ribeiro, A.J., Denisin, A.K., Wilson, R.E. & Pruitt, B.L. For whom the cells pull: Hydrogel and micropost devices for measuring traction forces. *Methods* **94**, 51-64 (2016).
26. Butler, J.P., Tolic-Norrelykke, I.M., Fabry, B. & Fredberg, J.J. Traction fields, moments, and strain energy that cells exert on their surroundings. *Am J Physiol Cell Physiol* **282**, C595-605 (2002).
27. Del Alamo, J.C. *et al.* Spatio-temporal analysis of eukaryotic cell motility by improved force cytometry. *Proc Natl Acad Sci U S A* **104**, 13343-13348 (2007).
28. Trepap, X. *et al.* Physical forces during collective cell migration. *Nature Phys* **5**, 426 (2009).
29. Ambrosi, D., Duperray, A., Peschetola, V. & Verdier, C. Traction patterns of tumor cells. *J Math Biol* **58**, 163-181 (2009).
30. Munoz, J.J. Non-regularised Inverse Finite Element Analysis for 3D Traction Force Microscopy. *International Journal of Numerical Analysis and Modeling* **13**, 763-781 (2016).
31. Sabass, B., Gardel, M.L., Waterman, C.M. & Schwarz, U.S. High resolution traction force microscopy based on experimental and computational advances. *Biophys J* **94**, 207-220 (2008).
32. Brask, J.B., Singla-Buxarra, G., Uroz, M., Vincent, R. & Trepap, X. Compressed sensing traction force microscopy. *Acta Biomater* **26**, 286-294 (2015).
33. Colin-York, H. *et al.* Super-Resolved Traction Force Microscopy (STFM). *Nano Lett* **16**, 2633-2638 (2016).
34. Bastounis, E. *et al.* Both contractile axial and lateral traction force dynamics drive amoeboid cell motility. *J Cell Biol* **204**, 1045-1061 (2014).
35. Hur, S.S., Zhao, Y., Li, Y.S., Botvinick, E. & Chien, S. Live Cells Exert 3-Dimensional Traction Forces on Their Substrata. *Cell Mol Bioeng* **2**, 425-436 (2009).
36. Toyjanova, J. *et al.* High resolution, large deformation 3D traction force microscopy. *PLoS One* **9**, e90976 (2014).
37. Maskarinec, S.A., Franck, C., Tirrell, D.A. & Ravichandran, G. Quantifying cellular traction forces in three dimensions. *Proc Natl Acad Sci U S A* **106**, 22108-22113 (2009).
38. Legant, W.R. *et al.* Measurement of mechanical tractions exerted by cells in three-dimensional matrices. *Nature methods* **7**, 969-971 (2010).
39. Steinwachs, J. *et al.* Three-dimensional force microscopy of cells in biopolymer networks. *Nature methods* **13**, 171-176 (2016).
40. Martiel, J.L. *et al.* Measurement of cell traction forces with ImageJ. *Methods in cell biology* **125**, 269-287 (2015).
41. Style, R.W. *et al.* Traction force microscopy in physics and biology. *Soft matter* **10**, 4047-4055 (2014).
42. Schwarz, U.S. & Soine, J.R. Traction force microscopy on soft elastic substrates: A guide to recent computational advances. *Biochim Biophys Acta* **1853**, 3095-3104 (2015).
43. Hutter, J.L. & Bechhoefer, J. Calibration of Atomic-Force Microscope Tips. *Review of Scientific Instruments* **64**, 1868-1873 (1993).
44. Tan, J.L. *et al.* Cells lying on a bed of microneedles: An approach to isolate mechanical force. *Proceedings of the National Academy of Sciences* **100**, 1484-1489 (2003).
45. du Roure, O. *et al.* Force mapping in epithelial cell migration. *Proceedings of the National Academy of Sciences* **102**, 2390-2395 (2005).
46. Gupta, M. *et al.* Adaptive rheology and ordering of cell cytoskeleton govern matrix rigidity sensing. *Nature communications* **6**, 7525 (2015).
47. Ghassemi, S. *et al.* Cells test substrate rigidity by local contractions on sub-micrometer pillars. *Proceedings of the National Academy of Sciences of the United States of America* **109**, 5328-5333 (2012).

48. Wolfenson, H. *et al.* Tropomyosin controls sarcomere-like contractions for rigidity sensing and suppressing growth on soft matrices. *Nature cell biology* **18**, 33-42 (2016).
49. Moore, S.W., Biais, N. & Sheetz, M.P. Traction on immobilized netrin-1 is sufficient to reorient axons. *Science* **325**, 166 (2009).
50. Biais, N., Higashi, D., So, M. & Ladoux, B. Techniques to measure pilus retraction forces. *Methods in molecular biology* **799**, 197-216 (2012).
51. Saez, A., Ghibaudo, M., Buguin, A., Silberzan, P. & Ladoux, B. Rigidity-driven growth and migration of epithelial cells on microstructured anisotropic substrates. *Proc Natl Acad Sci U S A* **104**, 8281-8286 (2007).
52. Lee, S., Hong, J. & Lee, J. Cell motility regulation on a stepped micro pillar array device (SMPAD) with a discrete stiffness gradient. *Soft matter* **12**, 2325-2333 (2016).
53. le Digabel, J. *et al.* Magnetic micropillars as a tool to govern substrate deformations. *Lab on a Chip* **11**, 2630-2636 (2011).
54. Sniadecki, N.J. *et al.* Magnetic microposts as an approach to apply forces to living cells. *Proceedings of the National Academy of Sciences of the United States of America* **104**, 14553-14558 (2007).
55. Ghibaudo, M. *et al.* Traction forces and rigidity sensing regulate cell functions. *Soft matter* **4**, 1836-1843 (2008).
56. Taubenberger, A.V., Hutmacher, D.W. & Muller, D.J. Single-cell force spectroscopy, an emerging tool to quantify cell adhesion to biomaterials. *Tissue engineering. Part B, Reviews* **20**, 40-55 (2014).
57. Bui, N., Durand-Smet, P. & Asnacios, A. Single-cell mechanics: the parallel plates technique. *Methods in cell biology* **125**, 187-209 (2015).
58. Harris, A.R. *et al.* Characterizing the mechanics of cultured cell monolayers. *Proceedings of the National Academy of Sciences* **109**, 16449-16454 (2012).
59. Rajagopalan, J. & Saif, M.T. MEMS Sensors and Microsystems for Cell Mechanobiology. *Journal of micromechanics and microengineering : structures, devices, and systems* **21**, 54002-54012 (2011).
60. Campas, O. *et al.* Quantifying cell-generated mechanical forces within living embryonic tissues. *Nat Meth* **11**, 183-189 (2014).
61. Serwane, F. *et al.* In vivo quantification of spatially varying mechanical properties in developing tissues. *Nature methods* **14**, 181-186 (2017).
62. Dolega, M.E. *et al.* Cell-like pressure sensors reveal increase of mechanical stress towards the core of multicellular spheroids under compression. *Nature communications* **8**, 14056 (2017).
63. Jurchenko, C. & Salaita, K.S. Lighting Up the Force: Investigating Mechanisms of Mechanotransduction Using Fluorescent Tension Probes. *Molecular and cellular biology* **35**, 2570-2582 (2015).
64. Meng, F., Suchyna, T.M. & Sachs, F. A fluorescence energy transfer-based mechanical stress sensor for specific proteins in situ. *The FEBS journal* **275**, 3072-3087 (2008).
65. Iwai, S. & Uyeda, T.Q. Visualizing myosin-actin interaction with a genetically-encoded fluorescent strain sensor. *Proc Natl Acad Sci U S A* **105**, 16882-16887 (2008).
66. Grashoff, C. *et al.* Measuring mechanical tension across vinculin reveals regulation of focal adhesion dynamics. *Nature* **466**, 263-266 (2010).
67. Austen, K. *et al.* Extracellular rigidity sensing by talin isoform-specific mechanical linkages. *Nature cell biology* **17**, 1597-1606 (2015).
68. Borghi, N. *et al.* E-cadherin is under constitutive actomyosin-generated tension that is increased at cell-cell contacts upon externally applied stretch. *Proceedings of the National Academy of Sciences* **109**, 12568-12573 (2012).

69. Cai, D. *et al.* Mechanical Feedback through E-Cadherin Promotes Direction Sensing during Collective Cell Migration. *Cell* **157**, 1146-1159.
70. Conway, D.E. *et al.* Fluid shear stress on endothelial cells modulates mechanical tension across VE-cadherin and PECAM-1. *Current biology : CB* **23**, 1024-1030 (2013).
71. Morimatsu, M., Mekhdjian, A.H., Adhikari, A.S. & Dunn, A.R. Molecular Tension Sensors Report Forces Generated by Single Integrin Molecules in Living Cells. *Nano Letters* **13**, 3985-3989 (2013).
72. Zhang, Y., Ge, C., Zhu, C. & Salaita, K. DNA-based digital tension probes reveal integrin forces during early cell adhesion. *Nature communications* **5**, 5167 (2014).
73. Blakely, B.L. *et al.* A DNA-based molecular probe for optically reporting cellular traction forces. *Nature methods* **11**, 1229-1232 (2014).
74. Chang, A.C. *et al.* Single Molecule Force Measurements in Living Cells Reveal a Minimally Tensioned Integrin State. *ACS Nano* (2016).
75. Woodside, M.T. *et al.* Nanomechanical measurements of the sequence-dependent folding landscapes of single nucleic acid hairpins. *Proc Natl Acad Sci U S A* **103**, 6190-6195 (2006).
76. Wang, X. & Ha, T. Defining single molecular forces required to activate integrin and notch signaling. *Science* **340**, 991-994 (2013).
77. Rahil, Z. *et al.* Nanoscale Mechanics Guides Cellular Decision Making. *Integrative Biology* (2016).
78. Galior, K., Liu, Y., Yehl, K., Vivek, S. & Salaita, K. Titin-Based Nanoparticle Tension Sensors Map High-Magnitude Integrin Forces within Focal Adhesions. *Nano Letters* **16**, 341-348 (2016).
79. Wang, N. *et al.* Cell prestress. I. Stiffness and prestress are closely associated in adherent contractile cells. *Am J Physiol Cell Physiol* **282**, C606-616 (2002).
80. Liu, Z. *et al.* Mechanical tugging force regulates the size of cell-cell junctions. *Proc Natl Acad Sci U S A* **107**, 9944-9949 (2010).
81. Maruthamuthu, V., Sabass, B., Schwarz, U.S. & Gardel, M.L. Cell-ECM traction force modulates endogenous tension at cell-cell contacts. *Proc Natl Acad Sci U S A* **108**, 4708-4713 (2011).
82. Ng, M.R., Besser, A., Brugge, J.S. & Danuser, G. Mapping the dynamics of force transduction at cell-cell junctions of epithelial clusters. *eLife* **3**, e03282 (2014).
83. Tambe, D.T. *et al.* Collective cell guidance by cooperative intercellular forces. *Nat Mater* (2011).
84. Lamason, R.L. *et al.* Rickettsia Sca4 Reduces Vinculin-Mediated Intercellular Tension to Promote Spread. *Cell* **167**, 670-683 e610 (2016).
85. Das, T. *et al.* A molecular mechanotransduction pathway regulates collective migration of epithelial cells. *Nature cell biology* **17**, 276-287 (2015).
86. Trepap, X. & Fredberg, J.J. Plithotaxis and emergent dynamics in collective cellular migration. *Trends in cell biology* **21**, 638-646 (2011).
87. Tambe, D.T. *et al.* Monolayer stress microscopy: limitations, artifacts, and accuracy of recovered intercellular stresses. *PLoS One* **8**, e55172 (2013).
88. Zimmermann, J. *et al.* Intercellular stress reconstitution from traction force data. *Biophys J* **107**, 548-554 (2014).
89. Nier, V. *et al.* Inference of Internal Stress in a Cell Monolayer. *Biophys J* **110**, 1625-1635 (2016).
90. Serra-Picamal, X., Conte, V., Sunyer, R., Muñoz, J.J. & Trepap, X. Chapter 17 - Mapping forces and kinematics during collective cell migration, in *Methods in Cell Biology*, Vol. Volume 125. (ed. K.P. Ewa) 309-330 (Academic Press, 2015).
91. Serra-Picamal, X. *et al.* Mechanical waves during tissue expansion. *Nat Phys* **8**, 628-634 (2012).
92. Soine, J.R. *et al.* Model-based traction force microscopy reveals differential tension in cellular actin bundles. *PLoS Comput Biol* **11**, e1004076 (2015).
93. Colombelli, J. *et al.* Mechanosensing in actin stress fibers revealed by a close correlation between force and protein localization. *Journal of Cell Science* **122**, 1665 (2009).

94. Grill, S.W., Gonczy, P., Stelzer, E.H.K. & Hyman, A.A. Polarity controls forces governing asymmetric spindle positioning in the *Caenorhabditis elegans* embryo. *Nature* **409**, 630-633 (2001).
95. Kumar, S. *et al.* Viscoelastic Retraction of Single Living Stress Fibers and Its Impact on Cell Shape, Cytoskeletal Organization, and Extracellular Matrix Mechanics. *Biophysical Journal* **90**, 3762-3773 (2006).
96. Fernandez-Gonzalez, R., Simoes, S.d.M., Röper, J.-C., Eaton, S. & Zallen, J.A. Myosin II Dynamics Are Regulated by Tension in Intercalating Cells. *Developmental Cell* **17**, 736-743.
97. Kasza, K.E., Farrell, D.L. & Zallen, J.A. Spatiotemporal control of epithelial remodeling by regulated myosin phosphorylation. *Proceedings of the National Academy of Sciences* **111**, 11732-11737 (2014).
98. Landsberg, K.P. *et al.* Increased Cell Bond Tension Governs Cell Sorting at the *Drosophila* Anteroposterior Compartment Boundary. *Current Biology* **19**, 1950-1955 (2009).
99. LeGoff, L., Rouault, H. & Lecuit, T. A global pattern of mechanical stress polarizes cell divisions and cell shape in the growing *Drosophila*. *Development* **140**, 4051 (2013).
100. Rauzi, M., Verant, P., Lecuit, T. & Lenne, P.-F. Nature and anisotropy of cortical forces orienting *Drosophila* tissue morphogenesis. *Nature cell biology* **10**, 1401-1410 (2008).
101. Porazinski, S. *et al.* YAP is essential for tissue tension to ensure vertebrate 3D body shape. *Nature* **521**, 217-221 (2015).
102. Campinho, P. *et al.* Tension-oriented cell divisions limit anisotropic tissue tension in epithelial spreading during zebrafish epiboly. *Nature cell biology* **15**, 1405-1414 (2013).
103. Davis, John R. *et al.* Inter-Cellular Forces Orchestrate Contact Inhibition of Locomotion. *Cell* **161**, 361-373.
104. Samarage, Chaminda R. *et al.* Cortical Tension Allocates the First Inner Cells of the Mammalian Embryo. *Developmental Cell* **34**, 435-447 (2015).
105. Bonnet, I. *et al.* Mechanical state, material properties and continuous description of an epithelial tissue. *Journal of The Royal Society Interface* **9**, 2614 (2012).
106. Hutson, M.S. *et al.* Forces for Morphogenesis Investigated with Laser Microsurgery and Quantitative Modeling. *Science* (2003).
107. Hutson, M.S. *et al.* Combining Laser Microsurgery and Finite Element Modeling to Assess Cell-Level Epithelial Mechanics. *Biophysical Journal* **97**, 3075-3085 (2009).
108. Kiehart, D.P., Galbraith, C.G., Edwards, K.A., Rickoll, W.L. & Montague, R.A. Multiple Forces Contribute to Cell Sheet Morphogenesis for Dorsal Closure in *Drosophila*. *The Journal of Cell Biology* **149**, 471 (2000).
109. Martin, A.C., Gelbart, M., Fernandez-Gonzalez, R., Kaschube, M. & Wieschaus, E.F. Integration of contractile forces during tissue invagination. *The Journal of Cell Biology* **188**, 735 (2010).
110. Scarcelli, G. *et al.* Noncontact three-dimensional mapping of intracellular hydromechanical properties by Brillouin microscopy. *Nature methods* **12**, 1132-1134 (2015).
111. Moeendarbary, E. *et al.* The cytoplasm of living cells behaves as a poroelastic material. *Nat Mater* **12**, 253-261 (2013).
112. Brodland, G.W. *et al.* CellFIT: A Cellular Force-Inference Toolkit Using Curvilinear Cell Boundaries. *PLoS ONE* **9**, e99116 (2014).
113. Chiou, K.K., Hufnagel, L. & Shraiman, B.I. Mechanical Stress Inference for Two Dimensional Cell Arrays. *PLoS Comput Biol* **8**, e1002512 (2012).
114. Guirao, B. *et al.* Unified quantitative characterization of epithelial tissue development. *eLife* **4**, e08519 (2015).
115. Ishihara, S. & Sugimura, K. Bayesian inference of force dynamics during morphogenesis. *Journal of Theoretical Biology* **313**, 201-211 (2012).



116. Sugimura, K. & Ishihara, S. The mechanical anisotropy in a tissue promotes ordering in hexagonal cell packing. *Development* **140**, 4091 (2013).
117. Veldhuis, J.H. *et al.* Inferring cellular forces from image stacks. *Philosophical Transactions of the Royal Society B* **372** (2017).
118. Etournay, R. *et al.* TissueMiner: A multiscale analysis toolkit to quantify how cellular processes create tissue dynamics. *eLife* **5** (2016).
119. Maitre, J.L. *et al.* Adhesion functions in cell sorting by mechanically coupling the cortices of adhering cells. *Science* **338**, 253-256 (2012).
120. Brodland, G.W. *et al.* Video force microscopy reveals the mechanics of ventral furrow invagination in *Drosophila*. *Proceedings of the National Academy of Sciences* **107**, 22111-22116 (2010).
121. Mayer, M., Depken, M., Bois, J.S., Julicher, F. & Grill, S.W. Anisotropies in cortical tension reveal the physical basis of polarizing cortical flows. *Nature* **467**, 617-621 (2010).
122. Sedzinski, J. *et al.* Polar actomyosin contractility destabilizes the position of the cytokinetic furrow. *Nature* **476**, 462-466 (2011).
123. Roca-Cusachs, P., Iskratsch, T. & Sheetz, M.P. Finding the weakest link - exploring integrin-mediated mechanical molecular pathways. *J. Cell Sci.* **125**, 3025-3038 (2012).
124. Alam, S., Lovett, D.B., Dickinson, R.B., Roux, K.J. & Lele, T.P. Nuclear forces and cell mechanosensing. *Progress in molecular biology and translational science* **126**, 205-215 (2014).
125. Han, M.K. & de Rooij, J. Converging and Unique Mechanisms of Mechanotransduction at Adhesion Sites. *Trends in cell biology* **26**, 612-623 (2016).
126. Chen, Y., Lee, H., Tong, H., Schwartz, M. & Zhu, C. Force regulated conformational change of integrin  $\alpha V\beta 3$ . *Matrix Biology* (2016).
127. Ehrlicher, A.J., Nakamura, F., Hartwig, J.H., Weitz, D.A. & Stossel, T.P. Mechanical strain in actin networks regulates FilGAP and integrin binding to filamin A. *Nature* **478**, 260-263 (2011).
128. Yao, M. *et al.* The mechanical response of talin. *Nature communications* **7** (2016).
129. Kong, F., Garcia, A.J., Mould, A.P., Humphries, M.J. & Zhu, C. Demonstration of catch bonds between an integrin and its ligand. *Journal of Cell Biology* **185**, 1275-1284 (2009).
130. Coste, B. *et al.* Piezo1 and Piezo2 are essential components of distinct mechanically activated cation channels. *Science* **330**, 55-60 (2010).
131. Wu, J., Goyal, R. & Grandl, J. Localized force application reveals mechanically sensitive domains of Piezo1. *Nature communications* **7**, 12939 (2016).
132. del Rio, A. *et al.* Stretching Single Talin Rod Molecules Activates Vinculin Binding. *Science* **323**, 638-641 (2009).
133. Yao, M. *et al.* Force-dependent conformational switch of alpha-catenin controls vinculin binding. *Nature communications* **5**, 4525 (2014).
134. Rivas-Pardo, J.A. *et al.* Work Done by Titin Protein Folding Assists Muscle Contraction. *Cell reports* **14**, 1339-1347 (2016).
135. Kinoshita, K., Leung, A., Simon, S. & Evans, E. Long-Lived, High-Strength States of ICAM-1 Bonds to  $\beta 2$  Integrin, II: Lifetimes of LFA-1 Bonds Under Force in Leukocyte Signaling. *Biophysical Journal* **98**, 1467-1475.
136. Ju, L., Chen, Y., Xue, L., Du, X. & Zhu, C. Cooperative unfolding of distinctive mechanoreceptor domains transduces force into signals. *eLife* **5** (2016).
137. Margadant, F. *et al.* Mechanotransduction in Vivo by Repeated Talin Stretch-Relaxation Events Depends Upon Vinculin. *PLoS Biol.* **9**, e1001223 (2011).
138. Klotzsch, E. *et al.* Fibronectin forms the most extensible biological fibers displaying switchable force-exposed cryptic binding sites. *Proceedings of the National Academy of Sciences of the United States of America* **106**, 18267-18272 (2009).

139. Kubow, K.E. *et al.* Mechanical forces regulate the interactions of fibronectin and collagen I in extracellular matrix. *Nature communications* **6** (2015).
140. Krieger, C.C. *et al.* Cysteine shotgun-mass spectrometry (CS-MS) reveals dynamic sequence of protein structure changes within mutant and stressed cells. *Proc.Natl.Acad.Sci.U.S.A* **108**, 8269-8274 (2011).
141. Yao, M. *et al.* Mechanical activation of vinculin binding to talin locks talin in an unfolded conformation. *Scientific reports* **4**, 4610 (2014).
142. Plotnikov, S.V., Pasapera, A.M., Sabass, B. & Waterman, C.M. Force fluctuations within focal adhesions mediate ECM-rigidity sensing to guide directed cell migration. *Cell* **151**, 1513-1527 (2012).
143. Elosegui-Artola, A. *et al.* Rigidity sensing and adaptation through regulation of integrin types. *Nature Materials* **13**, 631-637 (2014).
144. Lewis, A.H. & Grandl, J. Mechanical sensitivity of Piezo1 ion channels can be tuned by cellular membrane tension. *eLife* **4**, e12088 (2015).
145. Na, S. *et al.* Rapid signal transduction in living cells is a unique feature of mechanotransduction. *Proc.Natl.Acad.Sci.U.S.A* **105**, 6626-6631 (2008).
146. Case, L.B. *et al.* Molecular mechanism of vinculin activation and nanoscale spatial organization in focal adhesions. *Nature cell biology* **17**, 880-892 (2015).
147. Dupont, S. *et al.* Role of YAP/TAZ in mechanotransduction. *Nature* **474**, 179-183 (2011).
148. Roca-Cusachs, P., Gauthier, N.C., del Rio, A. & Sheetz, M.P. Clustering of  $\alpha 5\beta 1$  integrins determines adhesion strength whereas  $\alpha v\beta 3$  and talin enable mechanotransduction. *Proceedings of the National Academy of Sciences* **106**, 16245-16250 (2009).
149. Jiang, G.Y., Giannone, G., Critchley, D.R., Fukumoto, E. & Sheetz, M.P. Two-piconewton slip bond between fibronectin and the cytoskeleton depends on talin. *Nature* **424**, 334-337 (2003).
150. Seo, D. *et al.* A Mechanogenetic Toolkit for Interrogating Cell Signaling in Space and Time. *Cell* **165**, 1507-1518 (2016).
151. Mitrossilis, D. *et al.* Single-cell response to stiffness exhibits muscle-like behavior. *Proceedings of the National Academy of Sciences* **106**, 18243-18248 (2009).
152. Veldhuis, J.H., Mashburn, D., Hutson, M.S. & Brodland, G.W. Practical Aspects of the Cellular Force Inference Toolkit (CellFIT). *Methods in cell biology* **125**, 331-351 (2015).

Table 1

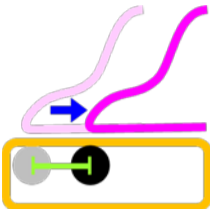

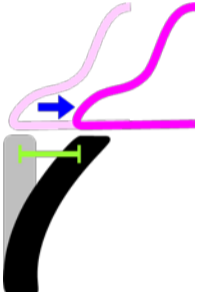
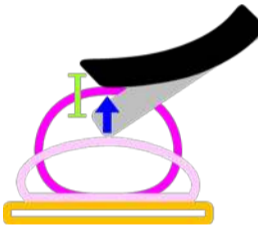
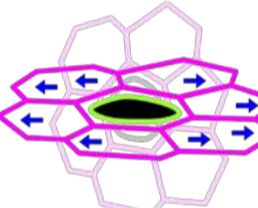
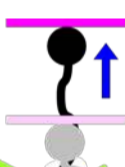
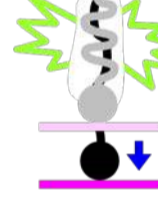
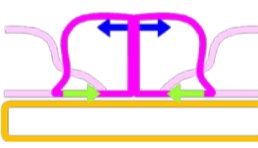
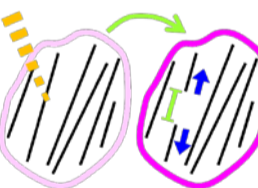
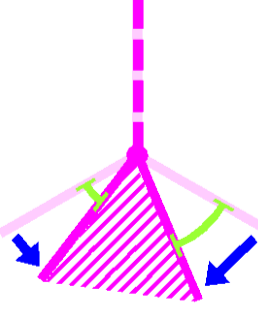
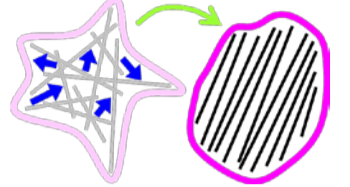
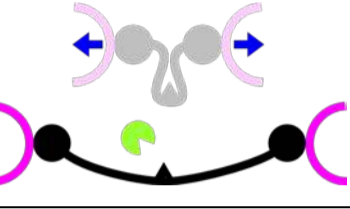
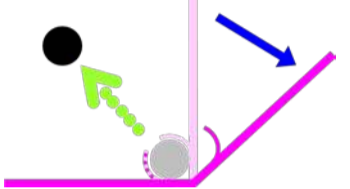
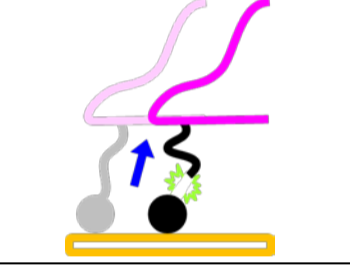
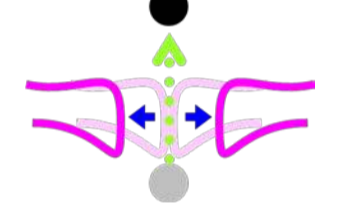
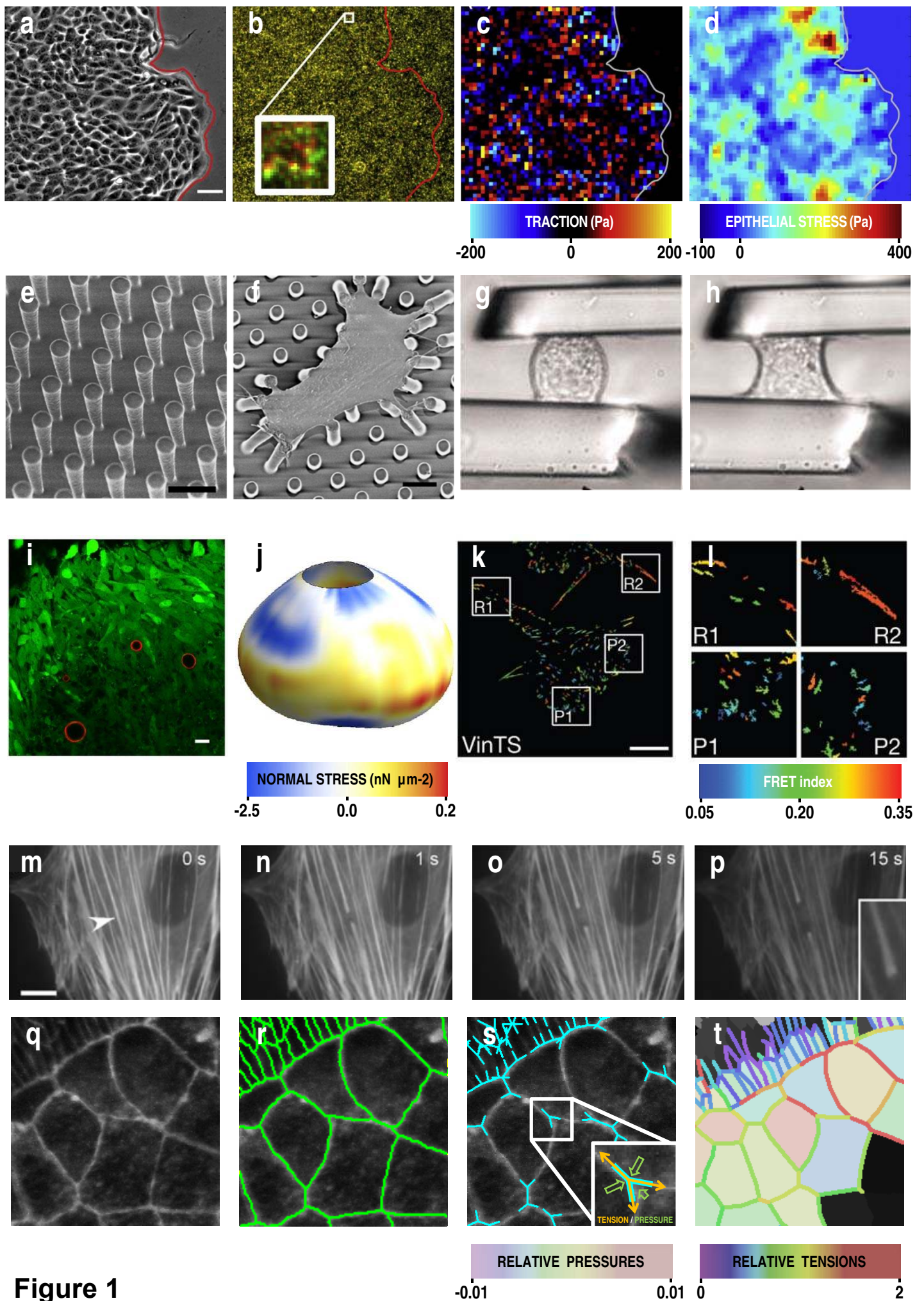
KNOWN MATERIAL PROPERTIES								
	Force range	Length scale	Measured quantity	In vivo?	Strengths	Limitations	Refs.	
2D Traction microscopy	$10^{-10^4}$ Pa	$10^{-1} - 10^3$ $\mu$ M	Substrate displacement	No	<ul style="list-style-type: none"> <li>Absolute measurement</li> <li>Tunability of substrate stiffness</li> <li>Output is a 2D map</li> </ul>	<ul style="list-style-type: none"> <li>Computationally involved</li> <li>High sensitivity to displacement noise</li> </ul>	21-42	
3D Traction microscopy	$10^{-10^4}$ Pa	$10^{-1} - 10^2$ $\mu$ M	ECM displacement	No	<ul style="list-style-type: none"> <li>Cells in 3D environment</li> <li>Output is a 3D map</li> </ul>	<ul style="list-style-type: none"> <li>Computationally very involved</li> <li>Unknown ECM material properties close to the cell</li> <li>Physiological ECM is non-linear.</li> </ul>	38, 39	
Micropillars	$10^{-2} - 10^2$ nN	$10^{-1} - 1$ $\mu$ M	Pillar displacement	No	<ul style="list-style-type: none"> <li>Absolute measurement</li> <li>No reference image required</li> <li>Simple force calculation</li> </ul>	<ul style="list-style-type: none"> <li>Discrete rather than continuous adhesion</li> <li>Difficulty to compare to physiological environments</li> <li>Small stiffness range</li> </ul>	44-54	
Cantilevers	$10^{-2} - 10^2$ nN	$10^{-1} - 10^3$ $\mu$ M	Cantilever displacement	No	<ul style="list-style-type: none"> <li>No reference image required</li> <li>Simple and precise force measurements in real time</li> </ul>	<ul style="list-style-type: none"> <li>Requires contact</li> <li>Low throughput</li> </ul>	56-59	
Inserts	$10^{-1} - 10^4$ Pa	$10^{-1} - 10^2$ $\mu$ M	Insert deformation	Yes	<ul style="list-style-type: none"> <li>In vivo</li> <li>Control of adhesion specificity</li> <li>Versatile</li> </ul>	<ul style="list-style-type: none"> <li>Requires microinjection</li> <li>No measurement of shear stress</li> <li>No measurement of isotropic stress</li> </ul>	60-62	
Molecular sensors – genetically encoded	1 – 10 pN	1 - 10 nm	Fluorescence signal	Yes	<ul style="list-style-type: none"> <li>Measures forces per molecule</li> <li>Molecular specificity</li> </ul>	<ul style="list-style-type: none"> <li>No directional information</li> <li>Difficult calibration</li> <li>Low signal-to-noise ratio</li> </ul>	64-70	
Molecular sensors – synthesized	1 – 100 pN	1 - 10 nm	Fluorescence signal	No	<ul style="list-style-type: none"> <li>Higher force range than genetically encoded</li> <li>Easier force calibration</li> </ul>	<ul style="list-style-type: none"> <li>Only available for extracellular ligands</li> </ul>	72-78	
UNKNOWN MATERIAL PROPERTIES								
Monolayer Stress Microscopy	$1 - 10^3$ nN	$1 - 10^3$ $\mu$ M	Unbalanced traction	No	<ul style="list-style-type: none"> <li>Exact solution in 1D</li> <li>Straightforward if tractions are known</li> </ul>	<ul style="list-style-type: none"> <li>Model assumption in 2D</li> </ul>	80-92	
Laser Ablation	NA	$0.1 - 10^3$ $\mu$ M	Wound deformation	Yes	<ul style="list-style-type: none"> <li>Multiscale</li> <li>Relatively simple implementation</li> <li>High precision of perturbation</li> </ul>	<ul style="list-style-type: none"> <li>Relative measurements</li> <li>Invasive</li> </ul>	93-109	
Force Inference	NA	$10^{-1} - 10^3$ $\mu$ M	Contour geometry	Yes	<ul style="list-style-type: none"> <li>Non-invasive</li> <li>No probe required (geometry only)</li> <li>Largely independent of material properties</li> </ul>	<ul style="list-style-type: none"> <li>Relative measurements</li> <li>Sensitive to image segmentation noise</li> </ul>	112-122	

Table 2

MECHANOTRANSDUCTION						
	Example molecule	Typical force	Length scale	Force-induced event	Refs.	
Cytoskeleton	Actin	1 nN	1 -10 $\mu$ m	Cytoskeletal remodelling	46	
Molecular extension	Integrin $\alpha$ V $\beta$ 3	10 pN	10 nm	Switch from bent to extended configuration	126	
Unfolding	Talin	1 pN	10 <sup>2</sup> nm	Unfolding of molecular domains	128	
Domain reorientation	Filamin	unknown	10 nm	Change in angle of dimer crosslinking, exposing integrin-binding sites	127	
Bond rupture	Integrin $\alpha$ 5 $\beta$ 1	10 pN	10 nm	Rupture of integrin-ECM bonds	129	
Opening of ion channels	Piezo1	10 pN	10 nm	Gating of ion channel	131	





**Figure 1**